

# Photocontrol of Cation Complexation with a Benzothiazolium Styryl Azacrown Ether Dye: Spectroscopic Studies on Picosecond and Kilosecond Time Scales

Igor K. Lednev,<sup>†</sup> Tian-Qing Ye, Ronald E. Hester, and John N. Moore\*

Department of Chemistry, The University of York, Heslington, York YO1 5DD, U.K.

Received: February 25, 1997; In Final Form: April 29, 1997<sup>⊗</sup>

UV–visible absorption and emission spectroscopy have been used to study the complexation of Ba<sup>2+</sup> with a benzothiazolium styryl azacrown ether dye and two derivatives, one without an azacrown and one with an alkylsulfonate pendant to the benzothiazolium group. Studies of the thermal *cis*–*trans* isomerization on the kilosecond time scale, and of the excited state leading to *trans*–*cis* photoisomerization on the picosecond time scale, are reported which enable a quantitative analysis of the kinetics and complexation equilibria to be obtained. The photophysics are interpreted by a scheme which includes rotation around both the olefinic C=C bond and adjacent C–C bonds in the excited state. A comparison of the data for this dye with those for other derivatives studied here and reported elsewhere indicates that the extent of intramolecular charge transfer in the excited state is a key factor in controlling the properties. An overall mechanism is proposed for the thermal and photochemical reactions of this dye which indicates that it is a good candidate for applications which require the photocontrolled complexation/release of barium cations in solution.

## Introduction

The incorporation of macrocyclic ionophores as ion-receptor and -carrier units within single molecules has received considerable attention of late and has stimulated extensive interest in the design and study of these molecules within supramolecular devices.<sup>1,2</sup> The variety of functional properties available from such systems has enabled ion-sensing devices such as ion-sensitive electrodes<sup>3–6</sup> and optodes<sup>4,7,8</sup> to be developed, and the design of triggered ion-capture, ion-release, and/or ion-transport molecular systems is of interest, in part because of their potential for application within molecular switching and memory storage devices.<sup>2,9</sup> Light is a particularly convenient trigger with which to control ion complexation,<sup>10</sup> and several photochemical processes have been used to form a new species with a cation affinity which is different from that of the starting compound, in both reversible<sup>10</sup> and irreversible<sup>11</sup> reactions. The photochemical processes used have included photoisomerization of spiropyrans, azobenzenes, and thioindigos,<sup>10,12–15</sup> photodimerization of anthracene,<sup>10</sup> and photocleavage of chelators and cryptands.<sup>11</sup>

Styryl dyes linked to crown ethers have been synthesized and studied because of the possibility of controlling ion complexation at the crown ether by photoisomerization of the styryl dye: for example, a benzothiazolium styryl dye containing a 15-crown-5 ether group has been shown to have a higher stability constant for complex formation with alkaline-earth metal cations in the *cis*-isomer than the *trans*-isomer form.<sup>16,17</sup> This effect was attributed to the formation of an additional intramolecular coordination between the crowned cation and an alkylsulfonate group pendant to the benzothiazolium dye, which is possible only for the *cis*-isomer. Our recent studies of derivatives in which a benzothiazolium styryl dye is linked to a monoazacrown have indicated that monoazacrown dyes may be particularly appropriate for the photocontrol of metal cation complexation for three reasons. First, the azacrown nitrogen is linked directly

to the dye and forms part of the extended  $\pi$ -conjugated system, shifting the long-wavelength absorption band into the more accessible visible region of the spectrum and giving stronger band shifts and stronger color changes on ion complexation than the normal crown ether analogues.<sup>18,19</sup> Second, monoazacrown ether dyes generally have moderate stability constants for complexation with metal cations<sup>19</sup> which should facilitate the photocontrol of higher cation concentrations than the normal crown ether analogues, for which high stability constants in both isomer forms preclude the release of a high concentration of cations. Third, we have found that an azacrown benzothiazolium styryl dye exhibits both ion-sensitivity and ion-selectivity in the thermal *cis*–*trans* isomerization following photoisomerization of the *trans*-isomer,<sup>20</sup> a feature which may be used in the development of thermoreversible photoionic molecular devices.

Picosecond time-resolved UV–visible absorption studies of metal complexes of monoazacrown ether derivatives of donor–acceptor stilbene-like molecules have shown that these complexes are less stable in the excited state than the ground state and that the interaction between the cation and the azacrown nitrogen atom is disrupted within ca. 10 ps of photolysis.<sup>11,21–24</sup> In these examples, the cation is recaptured as the excited state decays to regenerate the ground state, typically within <10 ns of photolysis.<sup>11</sup> In general, the use of photoisomerization to trigger ion release can be expected to be more effective than electronic excitation alone because the structural change which drives this release persists for the time scale of the thermal back-reaction to regenerate the *trans*-isomer, typically in the range of ca. 10<sup>1</sup>–10<sup>2</sup> s for azacrown ether benzothiazolium styryl dyes.<sup>18,20</sup>

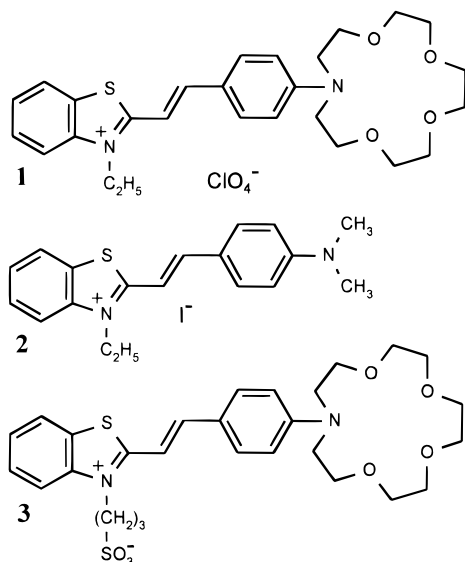
Here we report steady-state and time-resolved studies of the benzothiazolium styryl azacrown ether dye **1** and its interaction with barium cations. The aim of this study was to characterize the ion complexation properties of this dye quantitatively; this required kinetic studies of the excited-state photochemistry and the thermal back-reaction on picosecond and kilosecond time scales, respectively. In addition, we report parallel studies of one analogue with a pendant ethyl group but without an azacrown ether (**2**) and another analogue with both an azacrown

\* Corresponding author. Fax: +44(U.K.)-1904-432516. E-mail: jnm2@york.ac.uk.

<sup>†</sup> Current address: Chevron Science Center, Department of Chemistry, Box 39, University of Pittsburgh, Pittsburgh, PA 15260.

<sup>⊗</sup> Abstract published in *Advance ACS Abstracts*, June 15, 1997.

ether and a propylsulfonate group pendant to the dye (**3**) to enable the relative contributions of these moieties to the complexation properties to be explored.



## Experimental Section

The syntheses of **1** and **3** have been described.<sup>18,25</sup> **2**, acetonitrile (anhydrous), and Ba(ClO<sub>4</sub>)<sub>2</sub> (all Aldrich) were used as received. All studies were carried out at room temperature (ca. 18 °C).

A Hitachi U-3000 spectrophotometer and a Shimadzu RF-150X spectrofluorimeter were used for UV-visible absorption and emission studies, respectively, and samples were contained in 10-mm path length cells. A 250-W Xe lamp (XENOPHOT HLX 64655) and a 450-nm long-pass filter were used for steady-state photolysis. For the kinetic studies, the sample was photolyzed (ca. 1 min) and transferred immediately to the spectrometer, the lid closed, and the absorbance at a fixed wavelength measured as a function of time. Emission spectra were measured using perpendicular sampling geometry, and the sample concentrations were chosen to give an absorbance of ca. 0.06 at the excitation wavelength. Relative quantum yields of luminescence for different samples were estimated by measuring their spectra under identical conditions (sample absorbance, excitation power, and wavelength) and calculating the areas under the emission spectra. The emission spectra and quantum yields were obtained under conditions where the extent of sample photoisomerization was measured to be insignificant.

The ultrafast apparatus has been described in detail elsewhere.<sup>26,27</sup> Briefly, the output of an amplified dye laser system (606 nm, 50 μJ, 200 fs, 1050 Hz) was used to provide photolysis pulses by frequency doubling (303 nm, 1.4–1.8 μJ) and probe pulses by white light continuum generation. The continuum probe was split into two beams which were focused to a diameter of ca. 200 μm at two different positions in the sample cell. One probe beam was coincident with the photolysis beam, which was focused to a diameter of ca. 250 μm using near-collinear geometry. The emerging beams were analyzed using 10-nm band pass interference filters and photodiodes/lock-in amplifiers. In all cases, the relative polarization of the pump and probe beams was set at the “magic angle” of 54.7°. A stoppered 1-mm path length quartz cell containing the sample solution was translated rapidly in two directions perpendicular to the laser beams at a rate sufficient to ensure that each pulse pair encountered fresh sample.<sup>26</sup> UV-visible absorption spectra

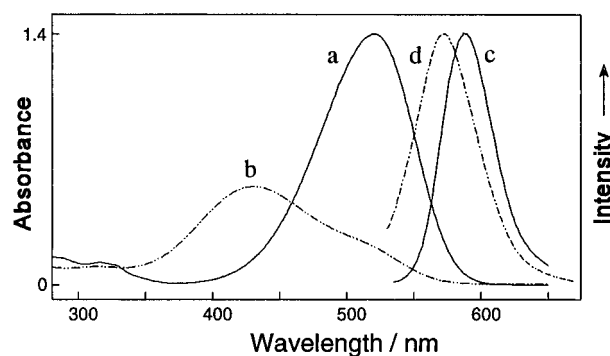


**Figure 1.** UV-visible spectra of **1** (ca.  $4 \times 10^{-5}$  M) in acetonitrile. Absorption spectra: (a) in the absence of added barium salt and (b) in the presence of Ba(ClO<sub>4</sub>)<sub>2</sub> at 0.88 M. Normalized emission spectra on 350 nm excitation: (c) in the absence of added barium salt and (d) in the presence of Ba(ClO<sub>4</sub>)<sub>2</sub> at 0.88 M.

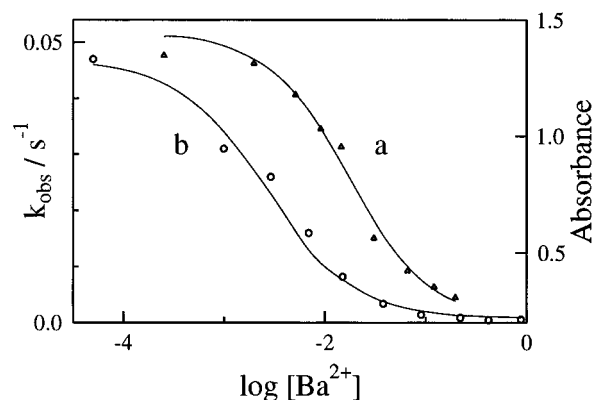


**Figure 2.** Ba(ClO<sub>4</sub>)<sub>2</sub> concentration dependence of (a) the absorbance of **1** at 520 nm, fitted to eq 1, and (b)  $k_{\text{obs}}$ , fitted to eq 8.

**TABLE 1: Absorption Maxima ( $\lambda_{\text{abs}}$ ), Fluorescence Emission Maxima ( $\lambda_{\text{f}}$ ), Excited State Lifetimes ( $\tau_{\text{e}}$ ), and Relative Quantum Yields of Fluorescence ( $\Phi_{\text{f}}^{\text{rel}}$ ) for the *trans*-Isomers of Dyes **1–3** in Acetonitrile Solution**

dye	$\lambda_{\text{abs}}/\text{nm}$	$\lambda_{\text{f}}/\text{nm}$	$\tau_{\text{e}}/\text{ps}$	$\Phi_{\text{f}}^{\text{rel}}$
<i>trans</i> - <b>2</b>	520	583	14	0.04
<i>trans</i> - <b>1</b>	520	582	39	0.20
<i>trans</i> - <b>1</b> -Ba <sup>2+</sup>	430	572	138	0.60
<i>trans</i> - <b>3</b>	522	583	205	1.00

measured before and after the laser experiments confirmed the integrity of the samples.

## Results

**Steady-State Absorption and Emission Spectroscopy.** The UV-visible absorption and emission spectra of *trans*-**1** in acetonitrile (Figure 1a,c) were found to be similar to those of *trans*-**2** and *trans*-**3** (Table 1). The absorptivities of these dyes are similar, but the quantum yields of luminescence were found to be significantly different, with relative values of  $\Phi_{\text{f}}^{\text{rel}} = 1.00$ , 0.20, and 0.04 for *trans*-**3**, **-1**, and **-2**, respectively (Table 1).

The absorption spectrum of *trans*-**1** in acetonitrile was measured as a function of Ba(ClO<sub>4</sub>)<sub>2</sub> concentration (Figure 2a), and the spectrum at [Ba(ClO<sub>4</sub>)<sub>2</sub>] = 0.88 M is shown in Figure 1b. The emission spectrum of this solution also was measured (Figure 1d); the quantum yield of luminescence was found to be ca. three times larger than that in the absence of Ba(ClO<sub>4</sub>)<sub>2</sub> (Table 1).

**Kinetics of Thermal *cis*–*trans*-Isomerization.** Styryl dyes such as **1–3** isomerize on photolysis, and the *cis*-isomers formed are thermally unstable and revert to the *trans*-isomers in the dark.<sup>18,20</sup> Solutions of **1** and **2** were irradiated with visible light

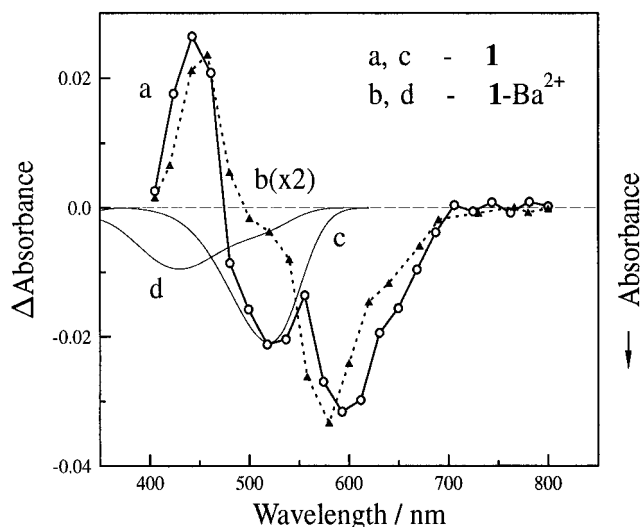


**Figure 3.** Time-resolved absorption spectra obtained 10 ps after 303-nm photolysis of **1** in acetonitrile: (a) **1** ( $3 \times 10^{-4}$  M) in the absence of added barium salt and (b) **1** ( $5 \times 10^{-4}$  M) in the presence of  $\text{Ba}(\text{ClO}_4)_2$  at 0.88 M. Ground-state absorption spectra of **1** in acetonitrile: (c) in the absence of added barium salt and (d) in the presence of  $\text{Ba}(\text{ClO}_4)_2$  at 0.88 M.

( $\lambda > 450$  nm) to generate a photostationary-state mixture containing the *cis*-isomer, and the kinetics of the *cis*–*trans* thermal isomerization were studied by measuring the absorbance at a fixed wavelength as a function of time after photolysis ceased. The kinetic data were found to fit well to a single-exponential function, giving a rate constant ( $k_{\text{obs}}$ ) corresponding to a lifetime ( $1/k_{\text{obs}}$ ) of  $\tau_f \approx 18$  s for *cis*-**1** in acetonitrile at room temperature. This lifetime increased substantially on addition of  $\text{Ba}(\text{ClO}_4)_2$ , and the kinetics were measured for several  $\text{Ba}(\text{ClO}_4)_2$  concentrations in the range ( $1 \times 10^{-4}$ )–0.88 M at a fixed concentration of **1** ( $5 \times 10^{-6}$  M). All of the kinetic data fit well to a single-exponential function, and thus the observed rate constant,  $k_{\text{obs}}$ , was obtained as a function of  $\text{Ba}^{2+}$  concentration (Figure 2b). In all cases the initial absorption spectrum recovered fully in the dark, on time scales of ca.  $10^1$ – $10^4$  s, dependent on the  $\text{Ba}^{2+}$  concentration.

The lifetime of *cis*-**2** in acetonitrile at room temperature was found to be ca. 10 s, and, in contrast to that of *cis*-**1**, it changed little on addition of  $\text{Ba}(\text{ClO}_4)_2$  up to a concentration of 0.16 M.

**Ultrafast Time-Resolved UV–Visible Spectroscopy.** The 303-nm photolysis of *trans*-**1** in acetonitrile solution resulted in a transient spectrum at 400–700 nm, as shown in Figure 3a for a delay time of 10 ps after the photolysis pulse. The kinetics of the transient signal were measured across this wavelength range, as illustrated for 442 and 620 nm (Figure 4a,b) for *trans*-**1**. A different transient spectrum (Figure 3b) and different kinetics (Figure 4e,f) were obtained on 303-nm photolysis of *trans*-**1** in acetonitrile in the presence of  $\text{Ba}(\text{ClO}_4)_2$  (0.88 M).

The 303-nm photolysis of *trans*-**2** and *trans*-**3** in acetonitrile solution resulted in transient spectra at 400–700 nm which were very similar to that of *trans*-**1**. The kinetics also were measured and are illustrated at 442 and 620 nm for *trans*-**2** (Figure 4c,d).

In all cases, the kinetics were found to fit well to a single exponential convoluted with the instrument response function, and the fitted lifetimes were found, within the error of the measurements, to be independent of probe wavelength for each solution. The excited state lifetimes,  $\tau_e$  ( $\pm 10\%$  error), clearly are different for each sample (Table 1).

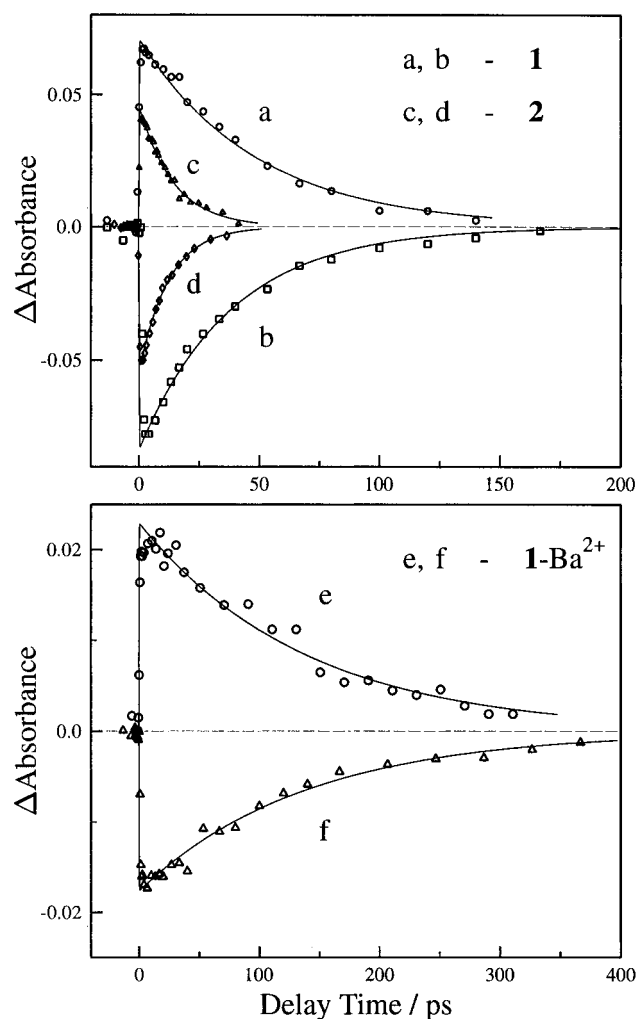


**Figure 4.**  $\Delta$ Absorbance signals obtained on 303-nm photolysis of **1**, **2**, and **1**- $\text{Ba}^{2+}$  in acetonitrile: **1** ( $2 \times 10^{-3}$  M) measured at (a) 442 and (b) 620 nm, **2** ( $2 \times 10^{-3}$  M) measured at (c) 442 and (d) 620 nm, and **1** ( $6 \times 10^{-4}$  M) in the presence of  $\text{Ba}(\text{ClO}_4)_2$  at 0.88 M measured at (e) 442 and (f) 580 nm. The solid lines are fits to a single-exponential function.

## Discussion

**$\text{Ba}^{2+}$  Complexation with *trans*-**1**.** The changes in the absorption spectrum of *trans*-**1** on addition of  $\text{Ba}(\text{ClO}_4)_2$  in acetonitrile solution are characteristic of ion complexation with the azacrown ether group of the chromoionophore,<sup>19,20</sup> and the spectrum in Figure 1b is assigned to *trans*-**1**- $\text{Ba}^{2+}$ . The dependence of the absorbance,  $A$ , at a fixed wavelength on the  $\text{Ba}^{2+}$  concentration may be described by eq 1, in accordance with the complexation reaction given as eq 2

$$A = [A_0 + (A_\infty K[M])]/[1 + (K[M])] \quad (1)$$



where  $A_0$  and  $A_\infty$  are the absorbances of the chromoionophore at zero and at infinite concentration, respectively, of the metal ion ( $[M]$ ),  $K$  is the stability constant of complex formation, and  $L$  and  $LM$  are the ligand (**1**) and the metal ion complex, respectively. The dependence of the absorbance at 520 nm on  $\text{Ba}^{2+}$  concentration in acetonitrile fits well to eq 1 (Figure 2a), giving a stability constant of  $K_{\text{trans}} = 80 \pm 15 \text{ M}^{-1}$  for *trans*-**1**- $\text{Ba}^{2+}$ . This is consistent with the value of  $70 \text{ M}^{-1}$  obtained for complexation of the azacrown of *trans*-**3** with  $\text{Ba}^{2+}$  in acetonitrile.<sup>19,20</sup>

**Thermal *cis*–*trans* Isomerization and Ba<sup>2+</sup> Complexation with *cis*-1.** The general scheme for the thermal back-reaction of *cis*–*trans* isomerization in the presence of metal ions in solution is given by eqs 3–6



where  $k_f$  and  $k_c$  are the rate constants of thermal *cis*–*trans* isomerization of **1** in free and cation-complexed forms, respectively, and  $K_{cis}$  and  $K_{trans}$  are the stability constants for complexation of *cis*- and *trans*-**1**, respectively, with Ba<sup>2+</sup>. The establishment of equilibria 5 and 6 will occur more rapidly than the thermal isomerization reactions 3 and 4, and therefore the system is at equilibrium, from the viewpoint of complexation, at all times during the dark reactions 3 and 4. For this condition, and assuming that only a small fraction of the metal cations are complexed (i.e. that the concentration of free cations is essentially equal to the total concentration of the salt), the kinetic equation for the dark reaction is

$$[cis-L]^\Sigma = [cis-L]_0^\Sigma \cdot \exp(-k_{obs}t) \quad (7)$$

where  $k_{obs}$  is the observed rate constant,  $t$  is the time after photolysis ceased,  $[cis-L]^\Sigma = [cis-L] + [cis-LM]$ ,  $[cis-L]_0^\Sigma = [cis-L]^\Sigma$  at time  $t = 0$ , and

$$k_{obs} = k_f/(1 + K_{cis}[M]) + k_c/[1 + (1/K_{cis}[M])] \quad (8)$$

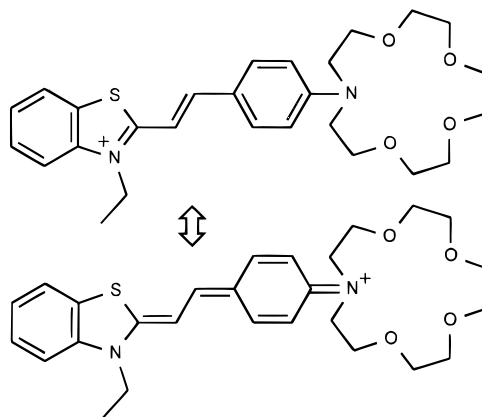
Equation 7 indicates that the kinetics of thermal *cis*–*trans* isomerization are monoexponential at any concentration of Ba<sup>2+</sup>, and eq 8 provides the actual rate constant as a function of Ba<sup>2+</sup> concentration. Equation 7 may be written in terms of the time-dependent absorbance ( $A_t$ ) at a fixed wavelength as

$$A_t = A_\infty + (A_0 - A_\infty) \cdot \exp(-k_{obs}t) \quad (9)$$

where  $A_0$  and  $A_\infty$  are the initial and final absorbances; eq 9 was used for analysis of the experimental data to obtain  $k_{obs}$ .

The observed dependence of  $k_{obs}$  on Ba<sup>2+</sup> concentration was found to fit well to eq 8 (Figure 2b), giving fitted values of  $K_{cis} = (360 \pm 40) \text{ M}^{-1}$ ,  $k_f = (0.06 \pm 0.02) \text{ s}^{-1}$ , and  $k_c = (4.8 \pm 0.3) \times 10^{-4} \text{ s}^{-1}$ . The fitted value of  $k_f$  is consistent with the lifetime of *cis*-**1** measured in the absence of Ba<sup>2+</sup>. The stability constant for Ba<sup>2+</sup> complexation with the *cis*-isomer,  $K_{cis}$ , is notably 4.5 times higher than that for Ba<sup>2+</sup> complexation with the *trans*-isomer.

The nitrogen atom within the azacrown ether group of **1** and **3**, or within the dimethylamino group of **2**, is also part of the  $\pi$ -conjugated system of the styryl dye. The molecular structures shown above each are one representation of these dyes, but a charge-transfer resonance form also contributes, resulting in a weakened olefinic C=C bond and a partial positive charge on the amino groups. We can use the relative contribution of this charge-transfer form to interpret the differences between the azacrown and normal crown ethers, between *cis*- and *trans*- forms of dyes **1**–**3**, and between different azacrown dyes.



The weakening of the central C=C bond explains the relative instability of the *cis*-isomers of **1**, **2**, and **3**, which undergo more rapid thermal *cis*–*trans* isomerization than dyes for which this resonance form has a smaller contribution; examples include benzothiazolium styryl dyes linked to normal crown ethers.<sup>16,17</sup> The relatively high partial positive charge on the azacrown nitrogen explains the lower stability constant of metal cation complexation for **1**, **2**, and **3** than for stilbene-based azacrown dyes,<sup>19</sup> consistent with the proposal that an increase in the electron-accepting ability of the chromophore within azacrown dyes results in a decrease in the electron density on the azacrown nitrogen and a lower stability constant for cation complexation.<sup>28</sup>

Resonance Raman studies have shown that *cis*-**3** has a higher wavenumber  $\nu(\text{C}=\text{C})$  band and hence a stronger central C=C bond than *trans*-**3**,<sup>18</sup> this difference being attributed to a smaller contribution of the charge-transfer resonance form in the *cis*-isomer which may arise from sterically induced nonplanarity weakening the  $\pi$ -conjugation through the chromophore. This effect may also explain the higher stability constant for cation complexation by *cis*-**1** than by *trans*-**1**: there is higher electron density at the azacrown nitrogen in the *cis*-isomer than the *trans*-isomer, resulting in stronger cation complexation. Similarly, the lower rate constant for thermal isomerization of *cis*-**1**-Ba<sup>2+</sup> than *cis*-**1** suggests that the presence of the cation within the azacrown further increases the electron density at the nitrogen, decreasing the contribution of the charge-transfer resonance form and increasing the strength of the central C=C bond.

The stability constant of  $K_{cis} = 2.7 \times 10^5 \text{ M}^{-1}$  that we have reported for the *cis*-**3**-Ba<sup>2+</sup> complex<sup>20</sup> is 750 times higher than that presented here for *cis*-**1**-Ba<sup>2+</sup>. We have attributed the high affinity of *cis*-**3** for Ba<sup>2+</sup> to the high equilibrium constant for SO<sub>3</sub><sup>-</sup>/Ba<sup>2+</sup> association in acetonitrile, which facilitates capture of the cation by the azacrown on isomerization.<sup>20</sup> The lower affinity for Ba<sup>2+</sup> complexation by *cis*-**1** quantifies the significance of the propylsulfonate group in this process. It is notable that, while the rate constant of  $k_f = 0.06 \text{ s}^{-1}$  for the thermal *cis*–*trans* isomerization of noncomplexed *cis*-**1** is similar to that of  $k_f = 0.04 \text{ s}^{-1}$  for *cis*-**3**, the rate constant of  $k_c = 4.8 \times 10^{-4}$  for the thermal isomerization of complexed *cis*-**1**-Ba<sup>2+</sup> is significantly lower than that of  $k_c = 3.5 \times 10^{-3} \text{ s}^{-1}$  for *cis*-**3**-Ba<sup>2+</sup>.<sup>20</sup> This indicates that, although intramolecular coordination of Ba<sup>2+</sup> to both the sulfonate and azacrown groups of **3** stabilizes the *cis*-isomer in comparison with the noncomplexed form, the complexed form without this additional “tail-biting” interaction that we have studied here, *cis*-**1**-Ba<sup>2+</sup>, is actually the more stable *cis*-isomer. The destabilization arising from the additional interaction of the propylsulfonate may result from steric strain, and it is possible that it would be lessened if a dye with a longer alkylsulfonate chain were used; the stability constant for complexation of alkaline-earth metal cations with benzothia-

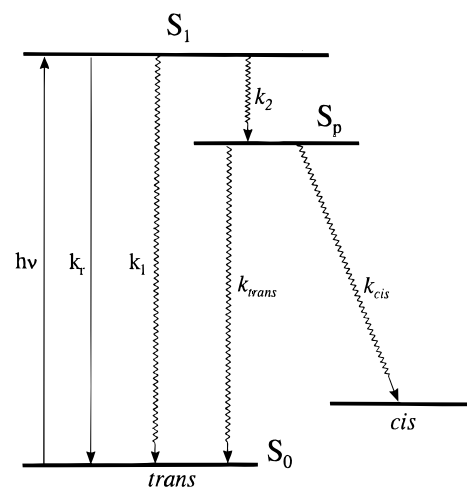
zolum styryl 15-crown-ether dyes has recently been reported to depend on the alkylsulfonate chain length.<sup>29</sup>

**Ultrafast Spectroscopy.** The ultrafast kinetic data fit well to a single-exponential decay in all cases and may be assigned to the decay of the  $S_1$  excited state of the respective dye. The transient spectrum of *trans*-**1** (Figure 3a), and similarly those of *trans*-**2** and **-3**, is attributable to the contribution of three components. First, the transient absorption at 400–480 nm may be attributed to the absorption of the  $S_1$  excited state of *trans*-**1**. Second, the bleach of the ground state absorption dominates at 480–550 nm, as is evident from a comparison of the transient spectrum (Figure 3a) with the normalized ground-state absorption spectrum of *trans*-**1** (Figure 3c). Third, the negative  $\Delta$ absorbance at 550–700 nm may be attributed to an increase in the intensity of the probe beam caused by stimulated emission from the dye: the profile of the steady-state emission spectrum (Figure 1c) is similar to that of this transient feature, and its kinetics are similar to those of both the excited-state absorption decay and the ground-state bleaching recovery, indicating that it arises from the  $S_1$  state. The transient spectrum arising from photolysis of *trans*-**1**-Ba<sup>2+</sup> (Figure 3b) comprises two strong features: transient absorption at 400–490 nm and stimulated emission at 540–700 nm. A weak feature at 490–540 nm may be attributed to bleaching of the ground-state absorption by comparison with the steady-state spectrum of *trans*-**1**-Ba<sup>2+</sup> (Figure 3d).

The lifetime of the excited state increases linearly with the relative quantum yield of fluorescence in the order **2**, **1**, **1**-Ba<sup>2+</sup>, and **3** (Table 1). The absorptivities of these dyes are similar, and so the simplest explanation of this trend is that the radiative rate constant is similar in each case and that the excited state lifetime and fluorescence quantum yield vary with changes in the rate constant for nonradiative decay of the excited state. One obvious candidate for a nonradiative decay mechanism is twisting around the central C=C bond, leading to photoisomerization. We have found that **1** and **3** undergo *trans*–*cis* photoisomerization efficiently in both free and cation-complexed forms, while **2** does so only at low yield.<sup>30</sup> If isomerization were the dominant nonradiative decay process for all of the dyes **1**–**3**, then the quantum yield for photoisomerization would be expected to be largest for **2**, which has the lowest quantum yield of fluorescence. We observe the reverse, and thus an additional mechanism of nonradiative decay is required to interpret the data.

Our observations suggest that the photophysics of **2** is similar to that reported for benzothiazolium LDS 751 (styryl **8**), which shows efficient  $S_1 \rightarrow S_0$  internal conversion which is faster than the radiative decay process.<sup>31</sup> This viscosity-dependent nonradiative process was tentatively assigned to free rotation around the C–C bonds between the polymethine chain and the end groups because the likely alternative mechanisms, of intersystem crossing to the triplet state and *trans*–*cis* photoisomerization, are inefficient for LDS 751.<sup>31</sup> Rotation around a single bond in the excited state, leading to a twisted intramolecular charge transfer (TICT) state, has been considered to be the main cause for the very short fluorescence lifetime of some stilbazolium and related pyridinium dyes at room temperature,<sup>32</sup> but there was no evidence for TICT state formation on photolysis of the styryl dyes studied here: only a single peak with a moderate Stokes shift was observed in the spontaneous and stimulated emission spectra, whereas dual emission with a large Stokes shift for the TICT state emission would be expected if a TICT state were formed. Again this is similar to LDS 751, where the absence of a TICT state has been explained by an excited-state structure in which partial charge transfer, from the

### SCHEME 1



dimethylanilino group to the benzothiazol group, results in delocalization of the positive charge over the entire molecule.<sup>31</sup> As a result, the Franck–Condon excited state of LDS 751 is much less polar than the ground state, and the steady-state fluorescence spectra vary little with solvent polarity. More recently, Strehmel and Rettig have suggested a photophysical scheme based on multiple excited states for dialkylamino stilbazolium dyes.<sup>32</sup> This scheme includes: a first-formed excited state which is relatively planar and shows radiative emission; twisting around the central C=C bond to give a nonradiative “phantom-singlet” state, leading to photoisomerization; twisting around two C–C bonds to give nonradiative charge-transfer states, which do not lead to photoisomerization; simultaneous twisting around C–C bonds and partial twisting around the C=C bond to give a state which returns to the ground state and gives no overall photoisomerization. This detailed scheme can be used to explain the photophysics of stilbene-like molecules, of donor–acceptor substituted stilbenes, and of the benzothiazolium styryl azacrown dyes studied here.

In the case of nonsubstituted stilbenes or stilbazolium salts, rotation around the central C=C bond is the dominant excited-state decay mechanism because this bond is weakened in the excited state. Rotation around C–C single bonds is an important decay mechanism for styryl and stilbene-like donor–acceptor dyes when there is strong intramolecular charge transfer along the polyene or ethylene chain in the excited state which gives less weakening of the central C=C bond (see resonance structures above).

In the case of the dyes studied here, this scheme can be adopted as illustrated in Scheme 1. This scheme gives three routes of decay from the *trans*- $S_1$  state: rotation around the central C=C bond ( $k_2$ ) to give a twisted state ( $S_p$ ) leading to photoisomerization, nonradiative decay by rotation around one or two C–C single bonds ( $k_1$ ), and radiative decay ( $k_r$ ). The UV–visible absorption and fluorescence spectra and the absorptivities of dyes **1**, **2**, and **3** are similar. If the radiative rate constant also is similar, then the quantum yield of fluorescence ( $\Phi_f$ ) will be proportional to the lifetime of the excited states ( $\tau_e$ ), varying with changes in  $k_1$  and  $k_2$ , as given by eqs 10 and 11. This linear correlation between  $\Phi_f$  and  $\tau_e$  is observed for dyes **1**–**3** (Table 1).

$$\Phi_f = k_r / (k_r + k_1 + k_2) \quad (10)$$

$$\tau_e = 1 / (k_r + k_1 + k_2) \quad (11)$$

The low quantum yields of both fluorescence and photoisomerization for **2** suggest that rotation of the dimethylami-

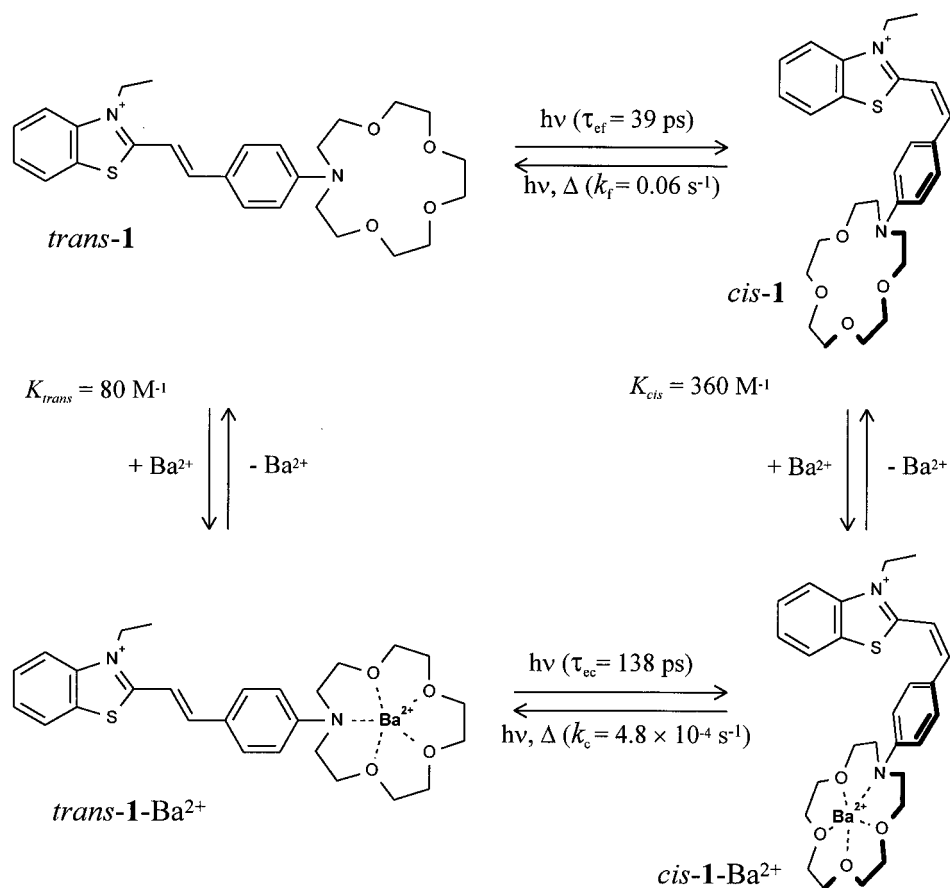


**Figure 5.** Proposed scheme for the photochemical ( $h\nu$ ) and thermal ( $\Delta$ ) reactions of **1** in acetonitrile, in the presence of  $\text{Ba}^{2+}$ , along with stability constants, lifetimes, and rate constants.

nophenyl and/or the benzothiazolium group around the respective C–C single bond dominates the decay of the excited state of **2**, i.e.  $k_1 > k_2, k_{\text{r}}$ . The higher quantum yields of fluorescence and photoisomerization for **1** suggest that rotation around these C–C single bonds occurs less readily and that  $k_1$  is lower for this dye: the bulky azacrown ether in **1** may be expected to inhibit this rotation in comparison with that of the dimethylamino group of **2**. There is a further increase in the quantum yields of fluorescence and photoisomerization in considering dye **3**, again attributable to a decrease in  $k_1$ , now arising from the bulkier propylsulfonate pendant to the benzothiazolium group.

The quantum yield of fluorescence and the lifetime of the excited state of **1** were found to increase by three times on complexation with  $\text{Ba}^{2+}$  (Table 1), following the same correlation described above for **1**, **2**, and **3**. Photoexcitation of several stilbene-like dyes containing a monoazacrown ether has been reported to result in intramolecular charge transfer, removing electron density from the azacrown nitrogen and breaking the nitrogen–cation bond;<sup>11,21–23</sup> in these cases, the cation remained complexed with the azacrown oxygen atoms, recombining to the nitrogen atom on decay of the excited state back to the ground state. Thus, photoexcitation of **1**- $\text{Ba}^{2+}$  similarly may result in intramolecular charge transfer, breakage of the azacrown N– $\text{Ba}^{2+}$  bond, and  $\text{Ba}^{2+}$  complexation with the azacrown oxygens. This proposal is in accordance with the observed spectra: both the steady-state fluorescence spectra and the time-resolved absorption spectra of **1** and **1**- $\text{Ba}^{2+}$  are similar, indicating that the electronic structures of the chromophores are similar in the excited state, while the ground-state absorption spectra are different (Figures 1 and 3), indicating that the cation interacts more strongly with the chromophore in the ground

state. If the  $\text{Ba}^{2+}$  ion is relatively remote from the chromophore in the excited state, then the excited-state decay mechanisms of **1**- $\text{Ba}^{2+}$  and **1** can be expected to be similar. The data suggest that both photoisomerization around the C=C bond and rotation around the single C–C bonds may contribute; the presence of  $\text{Ba}^{2+}$  within the azacrown renders this group more bulky than in the absence of  $\text{Ba}^{2+}$ , decreasing the nonradiative rate constants in accordance with Scheme 1.

Several aspects of this interpretation of the photophysics of dyes **1–3** are substantiated by additional reports in the literature. *trans*-4-(4-dimethylaminostyryl)-1-methylpyridiniumiodide<sup>32</sup> and (dibutylamino)stilbazolium butosulfonate<sup>33</sup> show a similar dependence of the photophysics on the size of the substituents: the quantum yields of both *trans*–*cis* photoisomerization and fluorescence are larger and the excited state lifetime is longer for the latter dye. Semiempirical quantum chemical calculations on stilbazolium dyes show that twisting of one or both of the C–C single bonds neighboring the olefinic double bond is energetically favorable in comparison with twisting of the dimethylamino group, which leads to a higher energy TICT state.<sup>34</sup> Rotation around a C–C single bond neighboring an olefinic double bond has been concluded to be preferable relative to twisting of the azacrown ether group around the phenyl–azacrown bond in the case of the  $\text{Ca}^{2+}$  complex of a stilbene-crown ether dye.<sup>28</sup>

**Overall Scheme for Photocontrolled  $\text{Ba}^{2+}$  Complexation and Release.** The scheme in Figure 5 summarizes the reactions occurring on photolysis of **1** in the presence of  $\text{Ba}^{2+}$  cations in solution. If the barium cation concentration is ca.  $3 \times 10^{-3} \text{ M}$ , then initially *trans*-**1** is present mainly in the noncomplexed (free) form. Visible wavelength photolysis results in *trans*–*cis* photoisomerization and subsequent complexation of the  $\text{Ba}^{2+}$

cations because the stability constant for complexation with *cis*-**1** is higher than that with *trans*-**1**. Ba<sup>2+</sup> complexation to *cis*-**1** can be expected to occur with a rate constant of  $\leq 10^8 \text{ M}^{-1} \text{ s}^{-1}$ ,<sup>35</sup> and therefore, at this Ba<sup>2+</sup> concentration, ion capture can be expected to occur on a time scale of  $\geq 3 \mu\text{s}$ . The captured cations are then released on a time scale of ca. 2 min (at this Ba<sup>2+</sup> concentration) after photolysis is ceased, as thermal isomerization regenerates *trans*-**1**. Therefore, this overall mechanism indicates that **1** combines the two useful properties of high-efficiency complexation on photolysis and subsequent release of the captured cations in the dark; such properties may be useful for the photocontrolled interphase transport of cations. It can be expected that the variation of the azacrown ether unit within this chromoionophore will result in different specificities and sensitivities to metal cations which will enable the design of molecules tailored for particular applications.

## Conclusion

This quantitative study of the Ba<sup>2+</sup> complexing properties of dyes **1**–**3**, and of their photochemistry on picosecond and kilosecond time scales, has enabled a detailed mechanism to be proposed for their thermal and photochemical ion-complexing reactions. The results presented here indicate that dyes such as **1** should be appropriate for photocontrolled ion-complexing applications, offering better opportunities for the photocontrol of cation release than more sophisticated dyes such as **3**, which offer better prospects for ion-sensing applications. Furthermore, these studies demonstrate that any azacrown ether linked to an acceptor dye, such as many examples of stilbene-based donor–acceptor azacrown dyes already reported in the literature, is potentially a photocontrolled ion-release system. This general molecular design meets the requirements of photoinduced charge transfer away from the azacrown nitrogen, which reduces the stability constant of the complex, and a structural change resulting from isomerization which maintains this change in stability constant over the relatively long time scale required for effective ion release. The experimental approach adopted in this study may usefully be extended to other cations and other dyes; such quantitative information on other molecules may be used, in particular, for quantitative comparisons which can inform strategies for the design of molecules tailored for particular applications.

**Acknowledgment.** We thank Dr. B. Strehmel for providing a copy of ref 34 prior to publication. We thank Professor M. V. Alfimov and Dr. O. A. Federova of the Photochemistry Department, Institute of Chemical Physics, the Russian Academy of Sciences, Moscow, for providing the samples of **1** and **3**. We acknowledge the support of DuPont and of EPSRC, the latter through a research grant and Advanced Fellowship (J.N.M.) awards.

## References and Notes

- Izatt, R. M.; Pawlak, K.; Bradshaw, J. S.; Bruening, R. L. *Chem. Rev.* **1995**, *95*, 2529.
- Lehn, J.-M. *Supramolecular Chemistry. Concepts and Perspectives*; VCH: Weinheim, 1995.
- Reinhoudt, D. N. *Recl. Trav. Chim. Pays-Bas* **1996**, *115*, 109.
- Wright, J. D. *Chem. Brit.* **1995**, *31*, 374.
- Pranitis, D. M.; Teltingdiaz, M.; Meyerhoff, M. E. *Crit. Rev. Anal. Chem.* **1992**, *23*, 16.
- Kimura, K.; Shono, T. In *Cation Binding by Macrocycles. Complexation of Cationic Species by Crown Ethers*; Inoue, Y., Gokel, G. W., Eds.; Marcel Dekker, Inc.: New York and Basel, 1990; Chapter 10, p 429.
- Alava-Moreno, F.; Pereiro-Garcia, R.; Diaz-Garcia, M. E.; Sanz-Medel, A. *Sens. Actuators* **1993**, *13*–*14*, 276.
- Lambeck, P. V. *Sens. Actuators* **1992**, *B8*, 103.
- Fabbrizzi, L.; Poggi, A. *Chem. Soc. Rev.* **1995**, 197.
- Shinkai, S. In *Cation Binding by Macrocycles. Complexation of Cationic Species by Crown Ethers*; Inoue, Y., Gokel, G. W., Eds.; Marcel Dekker, Inc.: New York and Basel, 1990; Chapter 9, p 397 and references therein.
- Valeur, B.; Bardez, E. *Chem. Brit.* **1995**, *31*, 216, and references therein.
- Kimura, K.; Yamashita, T.; Yokoyama, M. *J. Phys. Chem.* **1992**, *96*, 5614.
- Kimura, K.; Yamashita, T.; Yokoyama, M. *J. Chem. Soc., Perkin Trans. 2* **1992**, 613.
- Kimura, K.; Yamashita, T.; Yokoyama, M. *Chem. Lett.* **1991**, 965.
- Inouye, M.; Ueno, M.; Kitao, T.; Tsuchiya, K. *J. Am. Chem. Soc.* **1990**, *112*, 8977.
- Alfimov, M. V.; Gromov, S. P.; Lednev, I. K. *Chem. Phys. Lett.* **1991**, *185*, 455.
- Gromov, S. P.; Fyedorova, O. A.; Ushakov, E. N.; Stanislavsky, O. B.; Lednev, I. K.; Alfimov, M. V. *Dokl. Akad. Nauk SSSR* **1991**, *317*, 1134.
- Lednev, I. K.; Fyedorova, O. A.; Gromov, S. P.; Alfimov, M. V.; Moore, J. N.; Hester, R. E. *Spectrochim. Acta* **1993**, *49a*, 1055.
- Lednev, I. K.; Hester, R. E.; Moore, J. N. *J. Chem. Soc., Faraday Trans. 1997*, *93*, 1551 and references therein
- Lednev, I. K.; Hester, R. E.; Moore, J. N. *J. Am. Chem. Soc.* **1997**, *119*, 3456.
- Martin, M. M.; Plaza, P.; Meyer, Y. H.; Badaoui, F.; Bourson, J.; Lefevre, J.-P.; Valeur, B. *J. Phys. Chem.* **1996**, *100*, 6879.
- Martin, M. M.; Plaza, P.; Dai Hung, N.; Meyer, Y. H.; Bourson, J.; Valeur, B. *Chem. Phys. Lett.* **1993**, *202*, 425.
- Dumon, P.; Jonusauskas, G.; Dupuy, F.; Pee, P.; Rulliere, C.; Letard, J.-F.; Lapouyade, R. *J. Phys. Chem.* **1994**, *98*, 10391.
- Jonusauskas, G.; Lapouyade, R.; Delmond, S.; Letard, J. F.; Rulliere, C. *J. Chim. Phys.* **1996**, *93*, 1670.
- Alfimov, M. V.; Churakov, A. V.; Fedorov, Y. V.; Fedorova, O. A.; Gromov, S. P.; Hester, R. E.; Howard, J. A. K.; Kuz'mina, L. G.; Lednev, I. K.; Moore, J. N. Submitted for publication in *J. Chem. Soc., Perkin Trans. 2*.
- Ye, T. Q.; Arnold, C. J.; Pattison, D. I.; Anderton, C. L.; Dukich, D.; Perutz, R. N.; Hester, R. E.; Moore, J. N. *Appl. Spectrosc.* **1996**, *50*, 597.
- Lednev, I. K.; Ye, T.-Q.; Hester, R. E.; Moore, J. N. *J. Phys. Chem.* **1996**, *100*, 13338.
- Letard, J.-F.; Delmond, S.; Lapouyade, R.; Braun, D.; Rettig, W.; Kreissler, M. *Recl. Trav. Chim. Pays-Bas* **1995**, *114*, 517.
- Stanislavskii, O. B.; Ushakov, E. N.; Gromov, S. P.; Fedorova, O. A.; Alfimov, M. V. *Russ. Chem. Bull.* **1996**, *45*, 564.
- We estimated the relative quantum yields of *trans*–*cis* photoisomerization for **1**–**3** in two ways. First, while determining the rate of thermal *cis*–*trans* isomerization, we estimated the magnitude of  $\Delta A$  on photolysis using identical conditions for each dye (concentration, light intensity, geometry). **2** showed a much smaller change in absorbance than **1** or **3**. Second, in nanosecond flash photolysis studies to be reported elsewhere, we found no intermediate absorption with a lifetime longer than 2 ns for **1**, **2**, or **3**; we found only an immediate decrease in absorbance, at the long wavelength absorption peak, which persisted for several seconds. This change was largest for **3**, within the noise for **2**, and its magnitude is attributed to the extent of photoisomerization.
- Hebert, P.; Baldacchino, G.; Gustavsson, T.; Mialocq, J. C. *J. Photochem. Photobiol. A* **1994**, *84*, 45.
- Strehmel, B.; Rettig, W. *J. Biomed. Opt.* **1996**, *1*, 98 and references therein.
- Ephardt, H.; Fromherz, P. *J. Phys. Chem.* **1989**, *93*, 7717.
- Strehmel, B.; Seifert, H.; Rettig, W. *J. Phys. Chem. B* **1997**, *101*, 2232.
- Liesegang, G. W.; Eyring, E. M. In *Synthetic Multidentate Macrocyclic Compounds*; Izatt, R. M., Christensen, J. J., Eds.; Academic Press: New York, 1978; p 245.